

## Molecular Structure Features and Acid–Base Ionization of the 5–(4′–Aminophenyl)–10,15,20–tris(4′–sulfophenyl)porphine Conjugate with *H*–acid in Water

Vladimir B. Sheinin,<sup>a@</sup> Dmitriy A. Ivanov,<sup>a</sup> Olga M. Kulikova,<sup>a</sup> and Oscar I. Koifman<sup>a,b</sup>

<sup>a</sup>G.A. Krestov Institute of Solution Chemistry of Russian Academy of Sciences, 153045 Ivanovo, Russia

<sup>b</sup>Ivanovo State University of Chemistry and Technology, 153000 Ivanovo, Russia

@Corresponding author E-mail: vbs@isc-ras.ru

Using the DFT/B3LYP/6-31G(d,p) method, the relationship between molecular structure and acid-base properties of water-soluble conjugate obtained by azo coupling of the diazonium cation of 5-(4′-aminophenyl)-10,15,20-tris(4′-sulfonatophenyl)porphine with 1-amino-8-naphtholate-3,6-disulfonate (*H*-acid) in alkaline medium was analyzed. It was shown that a stable form of the pentanion of this azo compound is the hydrazone trans-tautomer with 1,2-quinoid structure of the *H*-fragment. The most acidic is hydrazone NNH-group, the dissociation of which begins in the region above pH 12 and can not be quantified. Dissociation of other weaker acid groups of the conjugate is limited by the upper value of the pH water scale. The pyrroline nitrogen atoms of the porphyrin platform  $H_2P$ , which diprotonates with close constants values, are most basic. It was shown that the reasons of synchronous  $H_2P$  diprotonation are the effects of substituents and the  $(H_2O)_2[H_4P^{2+}]$  aquacomplex formation, which act together. Further protonation of the *H*-fragment is limited by the lower value of pH water scale. The aquacomplex is an aggregation-stable zwitterion that does not form porphyrin J-aggregates even in the presence of self-assembly inducers. The reason for the high aggregation stability is the steric effect of the bulk *H*-fragment.

**Keywords:** Water-soluble azo dyes, meso-aminophenylporphine, meso-sulfophenylporphine, *H*-acid, azo-hydrazone tautomerism, protonation.

## Особенности молекулярного строения и кислотно–основная ионизация конъюгата 5–(4′–аминофенил)–10,15,20–трис(4′–сульфофенил)порфина с Аш–кислотой в воде

В. Б. Шейнин,<sup>a@</sup> Д. А. Иванов,<sup>a</sup> О. М. Куликова,<sup>a</sup> О. И. Койфман<sup>a,b</sup>

<sup>a</sup>Институт химии растворов им. Г.А. Крестова РАН, 153045 Иваново, Россия

<sup>b</sup>Ивановский государственный химико-технологический университет, 153000 Иваново, Россия

@E-mail: vbs@isc-ras.ru

Методом DFT/B3LYP/6-31G(d,p) проанализирована связь между молекулярным строением и кислотно-основными свойствами водорастворимого конъюгата, полученного азосочетанием катиона диазония 5-(4′-аминофенил)-10,15,20-трис(4′-сульфонатофенил)порфина с 1-амино-8-нафтолят-3,6-дисульфонатом (Аш-кислотой) в щелочной среде. Показано, что устойчивой формой пентаниона этого азосоединения является гидразонный транс-таутомер с 1,2-хиноидной структурой Аш-фрагмента. Самой кислой является гидразонная NNH-группа, диссоциация которой начинается в области выше pH 12 и не может быть охарактеризована количественно. Диссоциация других более слабых кислотных групп конъюгата ограничена верхней границей водной шкалы pH. Наибольшей основностью обладают пирролиновые атомы азота порфириновой платформы  $H_2P$ , которая дипротонируется с близкими значениями ступенчатых констант. Показано, что причиной синхронного дипротонирования  $H_2P$  являются эффекты заместителей и образование аквакомплекса  $(H_2O)_2[H_4P^{2+}]$ , которые действуют совместно. Дальнейшее протонирование Аш-фрагмента ограничено нижней границей водной шкалы pH. Аквакомплекс является агрегационно устойчивым цвиттер-

ионом, не образующим порфириновых *J*-агрегатов даже в присутствии индукторов самосборки. Причиной высокой агрегационной устойчивости является стерический эффект объемного Аш-фрагмента.

**Ключевые слова:** Водорастворимые азокрасители, мезо-аминофенилпорфин, мезо-сульфофенилпорфин, Аш-кислота, азо-гидразонная таутомерия, протонирование.

## Introduction

Water-soluble azo-conjugate based on 5-(4'-aminophenyl)-10,15,20-tris(4'-sulfonatophenyl)porphine and 1-amino-8-naphtholate-3,6-disulfonate (*H*-acid) is a new molecular platform promising for obtaining various functional compounds by multivariate modification of the porphyrin and/or *H*-acid unit. Porphyrin unit attracts interest due to possibility of metal derivatives and their axial complexes formation. *H*-Acid unit is available for further diazotization and azo coupling with the formation of extended azo-conjugates. In addition, the initial fragments and their potential derivatives possess the properties of ionic receptors, which is important for the design of supramolecular hybrid nanosystems. An important feature of the initial conjugate is the presence of five acid-base centers, the activity of which depends on *pH*, including, for example, azo-hydrazone tautomerism of the azo-bridge or the ability of sulfoporphyrins to form supramolecular zwitterionic *J*-aggregates. Presented work is devoted to the acid-base transformations analysis of azo-conjugate pentaanion in water.

## Experimental

**Reagents.** *H*-Conjugate was synthesized by azo coupling of diazonium cation of 5-(4'-aminophenyl)-10,15,20-tris(4'-sulfonatophenyl)porphine and 1-amino-8-naphtholate-3,6-disulfonate (*H*-acid) in alkaline medium, isolated and characterized by UV-Vis, <sup>1</sup>H NMR, MS-MALDI-TOF spectra in water as described in.<sup>[1]</sup>

5,10,15,20-(Tetraphenyl)porphine, 99 %, PorphyChem; *H*-acid (1-amino-8-naphtholate-3,6-disulfonate disodium salt), 99 %, Xian Health Biochem Technology Co., Ltd.; trifluoroacetic acid, 99 %, Panreac; sodium nitrate, reagent grade, JSC "Lenreaktiv"; aqueous ammonia 26 %, analytic grade, LLC "Sigma-Tech"; *n*-hexane, reagent grade, JSC "Lenreaktiv"; dichloromethane, reagent grade, LLC "Himmed"; hydrochloric acid 38 %, reagent grade, JSC "Lenreaktiv"; tin dihydrochloride, reagent grade, JSC "Lenreaktiv"; chloroform, reagent grade, LLC "Himmed"; sulfuric acid 95.6 %, reagent grade, CJSC "Vekton"; *n*-butanol, analytic grade, CJSC "Ekos-1"; sodium hydroxide, analytic grade, CJSC "Kaustic"; chitosan, Sigma Aldrich, 82 % degree of deacetylation; ε-polylysine, pure, Amtech Biotech Co., Ltd.

**Equipment.** NMR spectrometer Bruker Avance III 500, Bruker Biospin AG; mass-spectrometer Shimadzu Biotech AXIMA Confidence MALDI-TOF; fiber optic spectrophotometer-spectrofluorimeter AvaSpec-2048-2, equipped with temperature-controlled cell qpod® (Quantum Northwest); *pH*-meter 150 MI.

Quantum chemistry calculations were performed at the B3LYP/6-31++G(d,p) level of density functional theory using Gaussian software package.<sup>[2]</sup>

## Results and Discussion

Previously it has been shown that azo coupling of 5-(4'-aminophenyl)-10,15,20-tris(4'-sulfonatophenyl)

porphine diazonium cation with 1-amino-8-naphtholate-3,6-disulfonate in alkaline media leads to *H*-conjugate formation,<sup>[1]</sup> and its thermodynamically stable form (one of possible four, Figure 1S) is the hydrazone *trans*-tautomer with 1,2-quinoid structure of *H*-unit (Figure 1). *H*-Conjugate molecule is a porphyrin with multilayer system of substituents, which is convenient to consider as a "Russian doll" as the molecular structure becomes more complicated in the series (1)-**H<sub>2</sub>P**→(2)-**H<sub>2</sub>P**(Ph)<sub>4</sub>→(3)-**H<sub>2</sub>P**(PhNH<sub>2</sub>)(PhSO<sub>3</sub><sup>-</sup>)<sub>3</sub>→(4)-*H*-conjugate.

Unsubstituted porphyrin platform **H<sub>2</sub>P** has a planar structure due to four N-H...N bifurcate intramolecular hydrogen bonds (IMHB), which are 13 % shorter than the sum of van der Waals radii R<sub>w</sub>(H) and R<sub>w</sub>(N) (Table 1). Together with the aromatic porphyrin system, which tends to maintain the planarity, bifurcate IMHB completely compensate the intramolecular repulsion between two hydrogen atoms (IMHR), the distance between which is 5 % less than the sum 2R<sub>w</sub>(H). Hereinafter, we use the interatomic distance deviation from the sum of the van der Waals radii of atoms as a comparative criterion for hydrogen bonding and hydrogen repulsion.<sup>[3,4]</sup>

According to the second Etter's rule IMHB, which closing six-membered rings, have an advantage over intermolecular hydrogen bonds (IMHB) and thus completely block intracyclic atoms of the porphyrin platform from non-covalent intermolecular interactions.<sup>[3,4,8-13]</sup> Free rotation of phenyl rings is limited by van der Waals repulsion between their *ortho*-protons and β-protons of **H<sub>2</sub>P**. In **H<sub>2</sub>P**(Ph)<sub>4</sub>, the closest distance between *o*-H and β-H is only 0.8 Å, which is 64 % less than the sum of 2R<sub>w</sub>(H). Phenyl rings of **H<sub>2</sub>P**(Ph)<sub>4</sub> participate in the H-π-interaction with the porphyrin platform, as a result they rotate by ± 64° relative to the porphyrin *meso*-plane C5C10C15C20. This multiple H-π-interaction is the reason for the noticeable 1,3-alternation of the porphyrin platform **H<sub>2</sub>P**(Ph)<sub>4</sub> (Table 2), which distorts the initial planarity of **H<sub>2</sub>P** without weakening the bifurcated IMHB: pyrrole and pyrrolenine fragments alternately deviate from the *meso*-plane by a dihedral angle of ± 6°, and pyrrole atoms by - 0.05 Å. Three negative charged -SO<sub>3</sub><sup>-</sup> groups and one electron donating -NH<sub>2</sub> group are responsible for the enhancement of the H-π-interaction and decrease in the dihedral angles between the electron-rich substituted phenyl rings and the *meso*-plane **H<sub>2</sub>P**(PhNH<sub>2</sub>)(PhSO<sub>3</sub><sup>-</sup>)<sub>3</sub> to ± 59°.

*H*-Conjugate is a substitution product of one hydrogen atom at the amino group **H<sub>2</sub>P**(PhNH<sub>2</sub>)(PhSO<sub>3</sub><sup>-</sup>)<sub>3</sub>, where all the upper row atoms of *H*-unit and the amino group of porphyrin (Figure 1) are linked by strong intramolecular hydrogen bonds (IMHB), which close six-membered cycles and obey Etter's rules.<sup>[6,7]</sup> Due to hydrogen bonding, the *H*-fragment and the phenyl ring are in the coplanar position (Figure 2). Further, this coplanarity is preserved for all acid-base forms of *H*-conjugate considered in this work and is not commented on. Otherwise, the geometry of

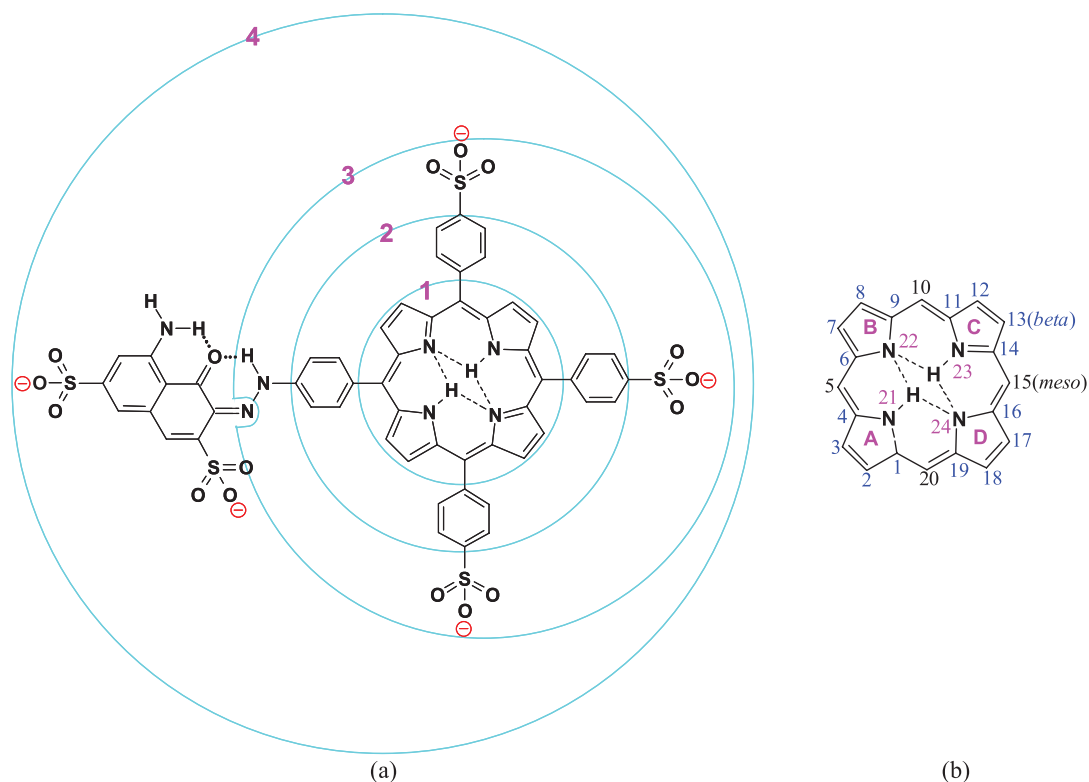


**Figure 1.** (a) – The structure and system of substituents of the *H*-conjugate with an increasing complexity of its chemical structure: (1) – porphine ( $H_2P$ ), (2) – 5,10,15,20-tetraphenylporphine ( $H_2P(Ph)_4$ ), (3) – 5-(4'-aminophenyl)-10,15,20-tris(4'-sulfonatophenyl)porphine, (4) – *H*-conjugate. (b) – Indexing of the porphyrin platform.

**Table 1.** Interatomic distance deviations from the sum of the van der Waals radii of atoms  $R_w^{[5]}$  (%).

Compound	IMHR						IMHB				
	$2R_w(H) - \text{distance HH}$						$R_w(H)+R_w(X) - \text{distance } X \cdots H$				
							$N \cdots H$				
AB	BC	CD	AD	AC	BD	AB	BC	CD	DA	$O \cdots H$	
$H_2P$					-5		-13	-13	-13	-13	-
$H_2P(Ph)_4$					-5		-13	-13	-13	-13	-
$H_2P(PhNH_2)(PhSO_3^-)_3$					-5		-12	-13	-12	-13	-
$H_2P$ in <i>H</i> -conjugate					-5		-13	-12	-13	-12	-
$H_3P^+$	-11	-11				-1			-17	-17	-
$H_3P^+(Ph)_4$	-6	-6				+2			-14	-14	-
$H_3P^+(PhNH_2)(PhSO_3^-)_3$	-4	-5				+3			-14	-13	-
$H_3P^+$ in <i>H</i> -conjugate	-4	-6				+4			-15	-12	-
$H_4P^{2+}$	-2	-2	-2	-2	15	15					-
$H_4P^{2+}(Ph)_4$	+8	+8	+8	+8	+22	+22					-
$H_4P^{2+}(PhNH_2)(PhSO_3^-)_3$	+7	+11	+13	+11	+25	+24					-
$H_4P^{2+}$ in <i>H</i> -conjugate	+13	+10	+5	+10	+24	+25					-
$(H_2O)_2H_4Por^{2+}$	+1	+1	+1	+1	+14	+14					-21*
$(H_2O)_2H_4P^{2+}(Ph)_4$	+8	+8	+8	+8	+20	+20					-21*
$(H_2O)_2H_4P^{2+}(PhNH_2)(PhSO_3^-)_3$	+8	+10	+12	+10	+22	+22					-20*
$(H_2O)_2H_4P^{2+}$ in <i>H</i> -conjugate	+15	+11	+6	+11	+24	+23					-19*

<sup>\*)</sup> average value

**Table 2.** Deviation of pyrrole, pyrrolenine, phenyl rings (dihedral angle) and intramolecular hydrogen atoms (distance) from the *meso*-plane of the porphyrin platform: sign (+) – upward deviation and (–) – downward deviation.

Platform	<i>meso</i> -plane	A	B	C	D	Ph*
	degree (°)					
<b>H<sub>2</sub>P</b>	0	0	0	0	0	–
<b>H<sub>2</sub>P(Ph)<sub>4</sub></b>	0	+5(–0.05)	–6	+5(–0.05)	–6	±64
<b>H<sub>2</sub>P(PhNH<sub>2</sub>)(PhSO<sub>3</sub><sup>–</sup>)<sub>3</sub></b>	0	+11(0.02)	–6	+6(+0.06)	–8	±59
<b>H<sub>2</sub>P in <i>H</i>-conjugate</b>	1	+6(–0.09)	–8	+7(–0.08)	–8	±59
<b>H<sub>3</sub>P<sup>+</sup></b>	0	+6(–0.25)	–12(+0.73)	+6(–0.25)	–3	–
<b>H<sub>3</sub>P<sup>+</sup>(Ph)<sub>4</sub></b>	0	+18(–0.37)	–22(+0.77)	+18(–0.37)	–15	±49
<b>H<sub>3</sub>P<sup>+</sup>(PhNH<sub>2</sub>)(PhSO<sub>3</sub><sup>–</sup>)<sub>3</sub></b>	1	+21(–0.43)	–24(+0.78)	+20(–0.37)	–19	±43
<b>H<sub>3</sub>P<sup>+</sup> in <i>H</i>-conjugate</b>	2	+20(–0.46)	–25(+0.76)	+19(–0.35)	–18	±43
<b>H<sub>4</sub>P<sup>2+</sup></b>	0	+16(–0.65)	–16(+0.65)	+16(–0.65)	–16(+0.65)	–
<b>H<sub>4</sub>P<sup>2+</sup>(Ph)<sub>4</sub></b>	0	+31(–0.76)	–31(+0.76)	31(–0.76)	–31(+0.76)	±33
<b>H<sub>4</sub>P<sup>2+</sup>(PhNH<sub>2</sub>)(PhSO<sub>3</sub><sup>–</sup>)<sub>3</sub></b>	0	+33(–0.74)	–34(+0.75)	35(–0.81)	–35(+0.81)	±26
<b>H<sub>4</sub>P<sup>2+</sup> in <i>H</i>-conjugate</b>		+34(–0.82)	–37(+0.81)	31(–0.72)	–32(+0.71)	±27
<b>(H<sub>2</sub>O)<sub>2</sub>H<sub>4</sub>Por<sup>2+</sup></b>	0	+14(–0.70)	–14(+0.70)	+14(–0.70)	–14(+0.70)	–
<b>(H<sub>2</sub>O)<sub>2</sub>H<sub>4</sub>P<sup>2+</sup>(Ph)<sub>4</sub></b>	0	+29(–0.78)	–29(+0.78)	+29(–0.78)	–29(+0.78)	±34
<b>(H<sub>2</sub>O)<sub>2</sub>H<sub>4</sub>P<sup>2+</sup>(PhNH<sub>2</sub>)(PhSO<sub>3</sub><sup>–</sup>)<sub>3</sub></b>	0	+32(–0.77)	–32(+0.77)	+34(–0.82)	–34(+0.82)	±27
<b>(H<sub>2</sub>O)<sub>2</sub>H<sub>4</sub>P<sup>2+</sup> in <i>H</i>-conjugate</b>	1	+36(–0.86)	–39(+0.85)	+31(–0.74)	–31(+0.73)	±26

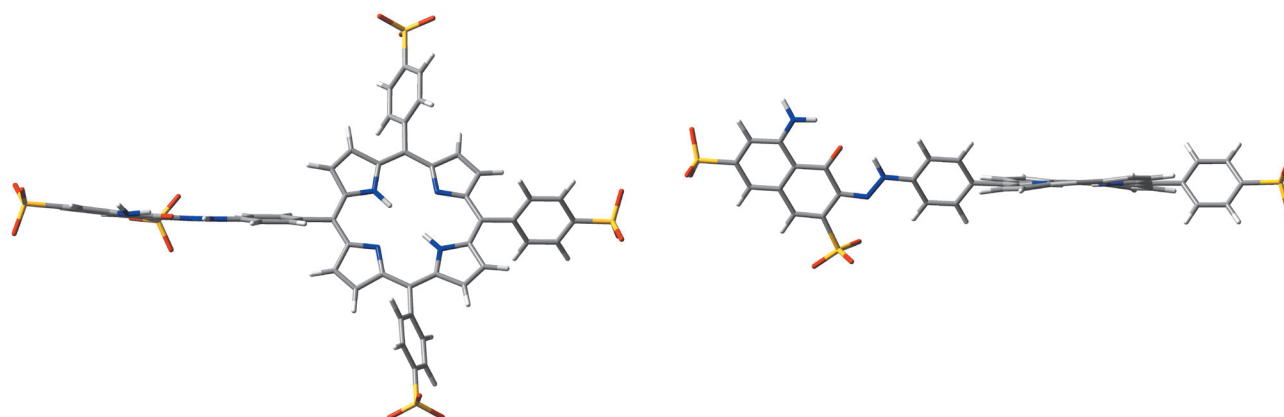
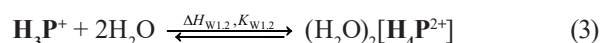
\*) average value

the *H*-conjugate porphyrin unit is little different from the precursor **H<sub>2</sub>P(PhNH<sub>2</sub>)(PhSO<sub>3</sub><sup>–</sup>)<sub>3</sub>**.

In the *H*-conjugate there is a number of different acid and base centers, connected by IMHB (Figure 1). The most acidic is the hydrazone NNH proton. The standard value of its dissociation DFT-enthalpy in the absence of a medium exceeds the alternative enthalpies of the first step acid dissociation of **H<sub>2</sub>P** and the amino group of the H-unit by 3.38 and 5.57 kcal/mol, respectively.

Hydrazone NNH-group is a very weak acid in aqueous solution, dissociation of which begins in *pH* range above 12

(Figure 3), and can be characterized quantitatively. Dissociation of other weaker acidic groups of the *H*-conjugate is limited by the upper value of the aqueous *pH* scale.

**Figure 2.** DFT-geometry of *H*-conjugate. In the left part, the phenyl rings perpendicular to the figure plane are omitted for clarity.

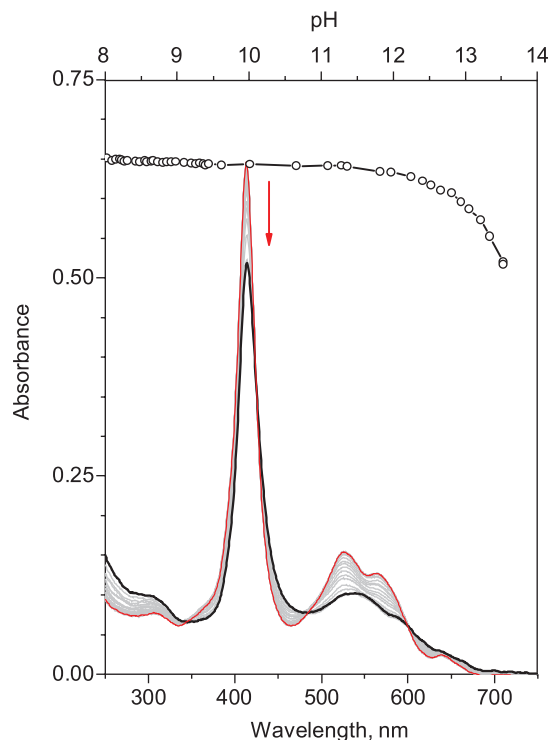


**Figure 3.** Changes in UV-Vis absorption spectra of *H*-conjugate as a result of hydrazone NNH-group acid dissociation in water at 25 °C.

$K_{B_2} = K_{b_2} \cdot K_{w_2} \cdot C_{H_2O}^2$ , where  $C_{H_2O}^2$  – concentration of water in water (55.42 mol/L at 25 °C).

Pyrroline nitrogen atoms of  $H_2P$  have the highest basicity in *H*-conjugate (Table 3).

First of them is protonated with a rapture of two bifurcate IMHBs and with a deepening of  $H_3P^+$  1,3-alternation in *H*-conjugate as a result of three protons IMHR enhancement, as well as the increasing of H- $\pi$ -interaction with the positively charged platform (Figure 4).

Hydrogen bonded rings A, C, and D deviate from the *meso*-plane by 19°, and their NH protons – approximately by 0.4 Å. Protonated pyrrole ring B, free from IMHB, deviates by 25° and its NH proton – by 0.76 Å. An excessive positive charge increases the H- $\pi$ -interaction of the  $H_3P^+$  in *H*-conjugate with electron-rich phenyl rings, as a result all dihedral angles with the *meso*-plane are reduced to 43°. The

H- $\pi$ -interaction is the reason that already in monoprotonated  $H_3P^+(Ph)_4$  IMHR disappears between the opposing protons 21 and 23, since the distance between them is 2 % higher than the  $2R_w(H)$  value. In  $H_3P^+$  of *H*-conjugate this value decreases to 4 % due to the substituents electronic effects. Nevertheless, despite the significant distortion of planarity, the acid-base centers of the monoprotonated porphyrin platform remain inaccessible for solvation and other non-covalent intermolecular interactions.<sup>[3,4,8–13]</sup> The substituents are responsible for the 69 % increase in the proton affinity of the *H*-conjugate  $H_2P$  unit with respect to porphine; 4 % of these belong to four phenyls, 46 % – to three sulfonate and one amino groups, and 19 % – to the H-fragment.

Protonation of the second pyrroline nitrogen atom leads to the complete destruction of bifurcate IMHB, as a result the  $H_4P^{++}$  got the elastic 1,3-alternate structure, where the porphyrin macrocycle distortion is balanced by the tendency of the aromatic system to planarity (Figure 5).

Due to the double positive charge and two pairs of converging NH-groups, the  $H_4P^{++}$  unit in *H*-conjugate possesses the molecular and anionic receptor properties with two interdependent sites of electrostatic and hydrogen bonding of “guests” located axially on opposite *meso*-plane sides. Average, dihedral angles between the *meso*-plane and pyrrole rings increase to  $\pm 34^\circ$ , with phenyl rings they decrease to  $\pm 27^\circ$ , and pyrrole NH atoms rise to a height of  $\pm 0.76$  Å. Strong H- $\pi$ -interaction between  $H_4P^{++}$  and electron-rich phenyl rings of *H*-conjugate is the reason for the increase in the average distance between the neighboring NH atoms by 10 % of the  $2R_w(H)$  value and, as a consequence, the complete absence of IMHR. It is known that in an aqueous solution, due to a large excess of water molecules acting as “guests”, porphyrin dication exists as aqua complex  $(H_2O)_2[H_4P^{++}]$ .<sup>[3,4,8–13]</sup> Sites of the  $H_4P^{++}$  platform of *H*-conjugate are pre-organized for efficient binding of  $H_2O$  oxygen atom in the aqua complex, where the N-H...O angle of intermolecular hydrogen bonds reaches 172°, approaching a right angle (Figure 6).

Positive charge leads to a decrease in the proton affinity of the  $H_3P^+$  in *H*-conjugate, but electron-donating effects of the substituents are increased. Proton affinity of  $H_3P^+$  in *H*-conjugate with respect to porphine increases already by 123 %, 16 % of them belong to four phenyls, 72 % – to three sulfonate and one amino groups, and 35 % – to H-fragment. As a result, this leads to a significant values convergence of

**Table 3.** DFT-enthalpies of reactions (1)-(4) in the absence of medium and corresponding constants in water at 25 °C.

Compound	$\Delta H_{b1}$	$\delta \Delta H_{b1}$	$\Delta H_{b2}$	$\delta \Delta H_{b2}$	$\Delta H_{b1} - \Delta H_{b2}$	$\Delta H_{b1} - (\Delta H_{b2} + \Delta H_{w1,2})$
	kcal/mol					
$H_2P$	-244.89		-164.08		-80.81	-42.11 (-48 %)
$H_2P(Ph)_4$	-255.91	-11.02 (+4 %)	-189.77	-25.69 (+16 %)	-66.14 (-18 %)	-32.14 (-60 %)
$H_2P(PhNH_2)(PhSO_3^-)_3$	-366.60	-121.71 (+50 %)	-308.17	-144.09 (+88 %)	-58.43 (-28 %)	-30.20 (-63 %)
$H_2P$ in <i>H</i> -conjugate	-414.71	-169.82 (+69 %)	-366.10	-202.02 (+123 %)	-48.61 (-40 %)	-22.84 (-72 %)

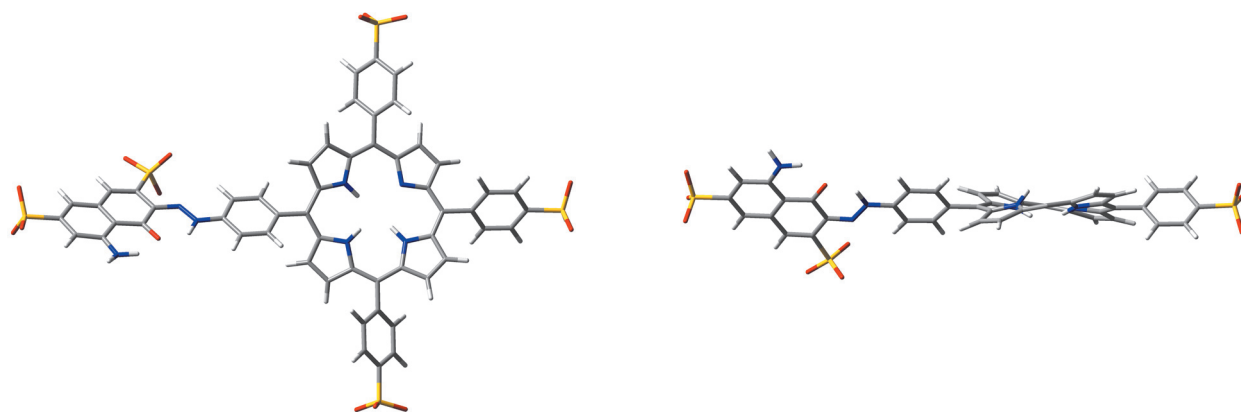


**Figure 4.** DFT-geometry of *H*-conjugate with  $\text{H}_3\text{P}^+$ . In the left part, the phenyl rings perpendicular to the figure plane are omitted for clarity.

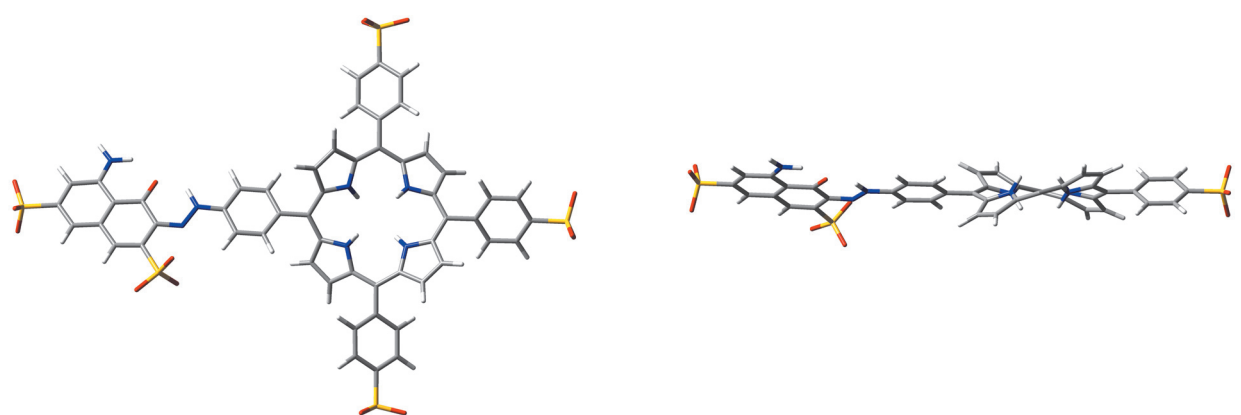


**Figure 5.** DFT-geometry of *H*-conjugate with  $\text{H}_4\text{P}^{2+}$ . In the left part, the phenyl rings perpendicular to the figure plane are omitted for clarity.

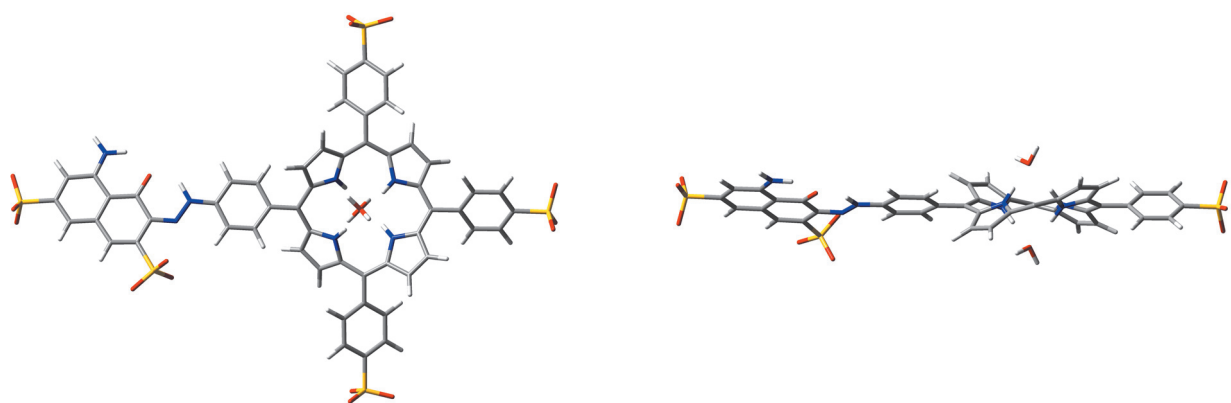


**Figure 6.** DFT-geometry of *H*-conjugate with  $(\text{H}_2\text{O})_2[\text{H}_4\text{P}^{2+}]$ . In the left part, the phenyl rings perpendicular to the figure plane are omitted for clarity.

the  $\text{H}_3\text{P}^+$  and  $\text{H}_2\text{P}$  proton affinities, the difference between them decreases to 60 %, and with the aqua complex formation – already to 28 %.

When diprotonated in water (Figure 7), these remaining differences (28 %) are almost completely leveled out due to the medium effect.

Aqua-complex  $(\text{H}_2\text{O})_2[\text{H}_4\text{P}^{2+}]$  formation is the reason of synchronous diprotonation of  $\text{H}_2\text{P}$  in *H*-conjugate with close values of step constants  $\lg K_{\text{b}1} = 5.31 \pm 0.01^{[1]}$  and  $\lg K_{\text{B}2} = 4.88 \pm 0.01^{[1]}$ , corresponds to the equations (1) and (4). As follows from equation (4) the  $K_{\text{B}2}$  value is the product of the second stage constant of the *H*-conjugate porphyrin

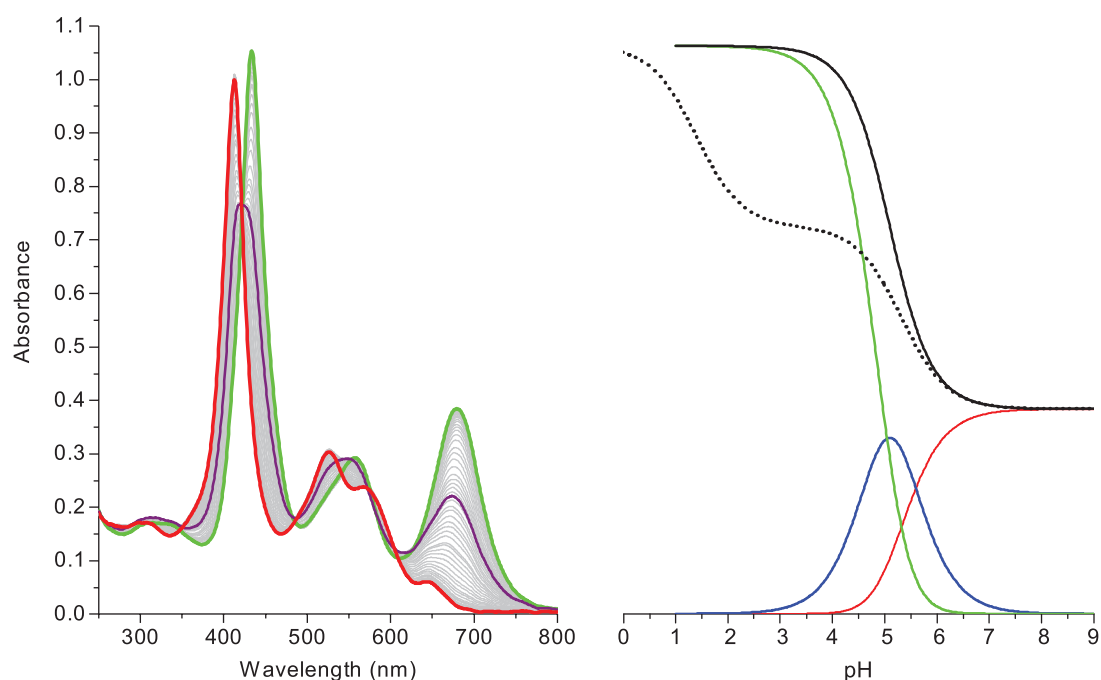


**Figure 7.** Changes in UV-Vis absorption spectra of the *H*-conjugate aqueous solution after addition of perchloric acid at 25° and corresponding changes in absorbance of the conjugated forms  $\mathbf{H}_2\mathbf{P}$  (red line),  $\mathbf{H}_3\mathbf{P}^+$  (blue line) and  $(\text{H}_2\text{O})_2[\mathbf{H}_4\mathbf{P}^{++}]$  (green line) at 434 nm. Purple line – spectrum of equilibrium mixture of these forms in the ratio of 28 %, 45 % and 27 %, respectively. Solid black line – experimental titration curve with  $K_{b1}$  and  $K_{B2}$ , dotted line – model titration curve, corrected for the medium effect  $C_{\text{H}_2\text{O}}^2$  with  $K_{b1}$  and  $(K_{b2} \cdot K_{w1,2})$ .

platform protonation  $\lg K_{b2}$  and the aqua-complex formation constant  $\lg K_{w1,2}$  multiplied by the square of the concentration of water in water, which can be conventionally taken as a constant value due to a large excess of solvent in relation to the reagents. Protonation of  $\mathbf{H}_2\mathbf{P}$  in water is accompanied by a transformation of the *H*-conjugate spectrum to the spectrum of the diprotonated form aqua complex  $(\text{H}_2\text{O})_2[\mathbf{H}_4\mathbf{P}^{++}]$  without fixing the spectrum of intermediate  $\mathbf{H}_3\mathbf{P}^+$  form, and the corresponding spectropotentiometric titration curves completely lose their stepwise character (Figure 7). Calculation using the equations (1)–(3) (SM) shows that the maximum concentration of monoprotinated *H*-conjugate under experimental conditions reaches only 45 % in an equilibrium mixture with 28 % of the neutral form and 27 % of the aqua complex (Figure 2S). Figure 7 presents the current absorbance values of these three conjugated forms, calculated by equations (5)–(7), the sum of which forms a smooth experimental titration curve obeying equation (8), with the constants  $\lg K_{b1}$  and  $\lg K_{B2}$ . Immediately the dotted line shows a model two-stage titration curve with the constants  $\lg K_{b1}$  and  $\lg K_{b2} \cdot \lg K_{w1,2}$ , which demonstrates the inductive medium effect in relation to two stages of *H*-conjugate porphyrin platform protonation due to the  $C_{\text{H}_2\text{O}}^2$  contribution.

$$A_{(\text{H}_2\text{P})}^{434\text{nm}} = \frac{A_{0(\text{H}_2\text{P})}}{1 + K_{b1} \cdot 10^{-\text{pH}} + K_{b1} \cdot K_{B2} \cdot 10^{-2\text{pH}}} \quad (5)$$

$$A_{(\text{H}_3\text{P}^+)}^{434\text{nm}} = \frac{A_{0(\text{H}_3\text{P}^+)} \cdot K_{b1} \cdot 10^{-\text{pH}}}{1 + K_{b1} \cdot 10^{-\text{pH}} + K_{b1} \cdot K_{B2} \cdot 10^{-2\text{pH}}} \quad (6)$$

$$A_{[(\text{H}_2\text{O})_2[\text{H}_4\text{P}^{++}]]}^{434\text{nm}} = \frac{A_{0[(\text{H}_2\text{O})_2[\text{H}_4\text{P}^{++}]]} \cdot K_{b1} \cdot K_{B2} \cdot 10^{-2\text{pH}}}{1 + K_{b1} \cdot 10^{-\text{pH}} + K_{b1} \cdot K_{B2} \cdot 10^{-2\text{pH}}} \quad (7)$$

$$A^{434\text{nm}} = \frac{A_{0(\text{H}_2\text{P})} + A_{0(\text{H}_3\text{P}^+)} K_{b1} 10^{-\text{pH}} + A_{0[(\text{H}_2\text{O})_2[\text{H}_4\text{P}^{++}]]} K_{b1} K_{B2} 10^{-2\text{pH}}}{1 + K_{b1} 10^{-\text{pH}} + K_{b1} K_{B2} 10^{-2\text{pH}}} \quad (8)$$

Aqua-complexes  $(\text{H}_2\text{O})_2[\mathbf{H}_4\mathbf{P}^{++}(\text{PhNH}_2)(\text{PhSO}_3^-)_3]$  and  $(\text{H}_2\text{O})_2[\mathbf{H}_4\mathbf{P}^{++}(\text{PhNH}_3^+)(\text{PhSO}_3^-)_3]$  are the monomers of zwitter-ionic *J*-aggregates, which are supramolecular polymers, self-assembled due to intramolecular substitution of water molecules by sulfonate groups of phenyl rings 5 and 15.<sup>[4,14]</sup> First *J*-aggregate can be produced at pH 4, and the second one at pH 1.<sup>[15]</sup> In general, porphyrin *J*-aggregates assembly is monitored by characteristic narrow *J*-bands, strongly shifted to the red region relative to the initial Soret and Q1-bands of the corresponding monomers.<sup>[1,14]</sup> The most characteristic is the Soret band shift to 490 nm (Figure 8(a)). Monomer of *H*-conjugate is not protonated in aqueous solution at the amino group of H-fragment and is not self-assembled into *J*-aggregates even in the presence of self-assembly inducers such as protonated chitosan or poly-*L*-lysine.

In acidic aqueous solutions, these polycations promote the convergence of monomers at a distance sufficient for their specific interaction due to electrostatic interaction with closely spaced positive charges.<sup>[4]</sup> For example, Figure 8(b) shows the absorption spectrum of the *H*-conjugate aqua complex in the presence of protonated poly-*L*-lysine ( $\text{p}K_b = 5$ ). The interaction of *H*-conjugate monomers with this cationic polyelectrolyte is accompanied only

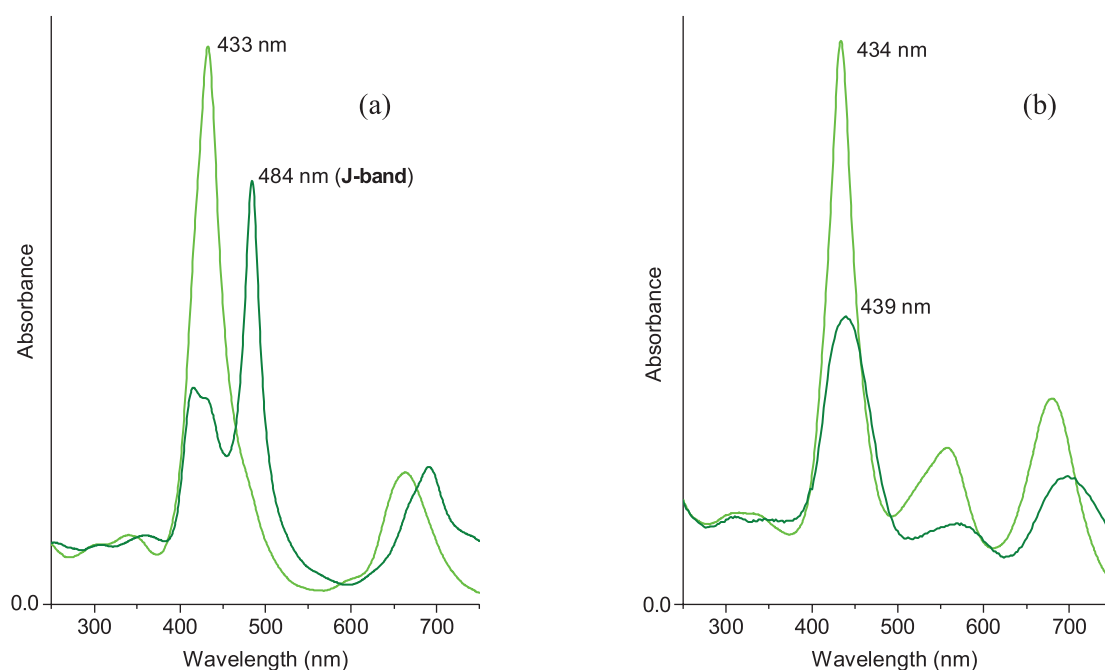


**Figure 8.** UV-Vis absorption spectra of aqua-complexes (green line) and aggregates (dark green line) for (a) –  $(\text{H}_2\text{O})_2[\text{H}_4\text{P}^{2+}(\text{PhNH}_3^+)(\text{PhSO}_3^-)_3]$  and (b) –  $H$ -conjugate with  $(\text{H}_2\text{O})_2[\text{H}_4\text{P}^{2+}]$ , in water (pH 1, 25 °C).

by broadening of absorption bands and a small 5 nm red shift of the Soret band, which is characteristic for ordinary aggregation.  $H$ -Conjugate and  $\text{H}_2\text{P}(\text{PhNH}_2)(\text{PhSO}_3^-)_3$  are characterized by close, almost identical values of stepwise protonation constants. For  $\text{H}_2\text{P}(\text{PhNH}_2)(\text{PhSO}_3^-)_3$ , the half-sum ( $\lg K_{\text{b1}} + \lg K_{\text{b2}}$ ) is  $5.06 \pm 0.02$ .<sup>[15]</sup> In addition, their aqua complexes also have similar geometry (Table 1,2). An obvious difficulty to the  $J$ -aggregates self-assembly from the  $H$ -conjugate aqua-complexes is the steric effect of the bulk  $H$ -fragment.

## Conclusions

Hydrazone *trans*-tautomer of the water-soluble azo-conjugate 5-(4'-aminophenyl)-10,15,20-tris(4'-sulfophenyl) porphine with  $H$ -acid is a  $pH$ -stable form of this compound in almost entire  $pH$  aqueous scale. Due to such structure, the porphyrin and the  $H$ -fragments are in a weak electronic interaction. Steric effect of bulky  $H$ -fragment inhibits the  $pH$ -dependent self-assembly of these sulfoporphyrin zwitterions into  $J$ -aggregates. This combination of chemical properties opens up the perspective of obtaining new water-soluble compounds, based on this platform, with the expected physicochemical and supramolecular functionality, as well as various bis- and multiporphyrin molecular systems using standard approaches developed for each fragment.

**Acknowledgements.** Presented work was supported by Russian Foundation for Basic Research according to the research project No. 18-33-01025.  $^1\text{H}$  NMR and MS MALDI-

TOF measurements were made in the centre for joint use of scientific equipment “The upper Volga region centre of physico-chemical research”.

## References

- Ivanov D.A., Sheinin V.B., Lyubimtsev A.V., Kulikova O.M., Koifman O.I. *Macroheterocycles* **2019**, *12*, 375–381.
- Frisch M.J., Trucks G.W., Schlegel H.B., *et al.* *Gaussian 09* (Gaussian, Inc., Wallingford CT, **2009**).
- Sheinin V.B., Kulikova O.M., Koifman O.I. *Macroheterocycles* **2018**, *11*, 363–370.
- Sheinin V.B., Kulikova O.M., Koifman O.I. *J. Mol. Liq.* **2019**, *277*, 397–408.
- Batsanov S.S. *Inorg. Mater.* **2001**, *37*, 871–885.
- Etter M.C. *Acc. Chem. Res.* **1990**, *23*, 120–126.
- Steed J.W., Atwood J.L. *Supramolecular Chemistry*. Chichester: J. Wiley&Sons Ltd., **2000**. 745 p.
- Sheinin V.B., Ivanova Y.B., Berezin B.D. *Russ. J. Coord. Chem.* **2002**, *28*, 149–151.
- Sheinin V.B., Ivanova Y.B., Berezin B.D. *Russ. J. Gen. Chem.* **2002**, *72*, 1128–1131.
- Sheinin V.B., Simonova O.R., Ratkova E.L. *Macroheterocycles* **2008**, *1*, 72–78.
- Sheinin V.B., Ratkova E.L., Mamardashvili N.Zh. *J. Porphyrins Phthalocyanines* **2008**, *12*, 1211–1219.
- Sheinin V.B., Shabunin S.A., Bobritskaya E.V., Koifman O.I. *Macroheterocycles* **2011**, *4*, 80–84.
- Sheinin V.B., Shabunin S.A., Bobritskaya E.V., Ageeva T.A., Koifman O.I. *Macroheterocycles* **2012**, *5*, 252–259.
- Sheinin V.B., Bobritskaya E.V., Shabunin S.A., Koifman O.I. *Macroheterocycles* **2014**, *7*, 209–217.
- Zurita A., Duran A., Ribo J.M., El-Hachemi Z., Crusats J. *SC Adv.* **2017**, *7*, 3353–3357.

Received 25.03.2020

Accepted 13.10.2020